Relativistic Generation of Isolated Attosecond Pulses in a λ^3 Focal Volume

N. M. Naumova,[1,*] J. A. Nees,[1] I. V. Sokolov,[2] B. Hou,[1] and G. A. Mourou[1,†]

[1]*Center for Ultrafast Optical Science, University of Michigan, Ann Arbor, Michigan 48109-2099, USA*
[2]*Space Physics Research Laboratory, University of Michigan, Ann Arbor, Michigan 48109-2143, USA*

(Received 6 May 2003; published 12 February 2004; publisher error corrected 13 February 2004)

Lasers that provide an energy encompassed in a focal volume of a few cubic wavelengths (λ^3) can create relativistic intensity with maximal gradients, using minimal energy. With particle-in-cell simulations we found, that single 200 attosecond pulses could be produced efficiently in a λ^3 laser pulse reflection, via deflection and compression from the relativistic plasma mirror created by the pulse itself. An analytical model of coherent radiation from a charged layer confirms the pulse compression and is in good agreement with simulations. The novel technique is efficient ($\sim 10\%$) and can produce single attosecond pulses from the millijoule to the joule level.

DOI: 10.1103/PhysRevLett.92.063902 PACS numbers: 42.65.Re, 52.25.Os, 52.27.Ny, 52.65.Rr

The generation of subfemtosecond pulses has been proposed [1] and demonstrated [2] using laser atom interaction in the nonperturbative regime in gases at intensities of the order of 10^{14} W/cm^2. In this domain attosecond pulses may be generated, but even with quasi-periodic phase matching [3] produce efficiency far below a percent. It may, however, be possible that higher intensity coupled with dense plasma and relativistic effects could generate attosecond pulses with very high efficiency.

We have recently produced relativistic intensity in the kHz regime with short pulses of less than 10 fs [4], composed of only a few cycles, focused on a single wavelength spot size [5]. In this case, the entire laser pulse energy is contained within a focal volume of few λ^3. This has become known as the λ^3 regime.

Driven relativistically, electrons acquire a quiver energy exceeding their rest mass energy $m_e c^2$. When considering relativistic laser interactions, it is convenient to express intensity in terms of the normalized vector potential $a_0 = e|A|/m_e c^2$. With $a_0 > 1$ corresponding to intensities above 2×10^{18} W/cm^2 for 0.8 μm light, the plasma dielectric constant must take relativistic effects into account. Accordingly, $\epsilon = 1 - \omega_{p0}^2/\gamma\omega^2$, where $\gamma = (1 + a_0^2)^{1/2}$ with $\omega_{p0} = (4\pi n_{e0} e^2/m_e)^{1/2}$.

The relativistic effect on ϵ has mainly been studied in subcritical density plasmas conditions, that is in *refraction* — commonly known as relativistic self-focusing — where the laser wave front is modified due to the dielectric constant dependence on a_0. This effect was discussed by Litvak [6] and Max *et al.* [7]. It was observed with excimer lasers [8] and with CPA lasers [9]. Mourou *et al.* [10] proposed, that this effect could be studied in the λ^3 regime, provided that the numerical aperture of the relativistic filament is matched with that of the focusing optics. This regime has the advantage that it requires only millijoule energies which are easily produced at kilohertz repetition rates [2–5].

We suggest that the concept of the relativistic self-focusing be extended from *refraction* to *reflection and deflection* for the case when the λ^3 laser pulse interacts with an overcritical density plasma. For $a_0 > 1$ the light pressure can significantly modify the shape and motion of the reflecting surface of the plasma which in turn will change the reflected wave front. We discovered by particle-in-cell (PIC) simulations that the plasma mirror produced by the laser pulse can be *deflective* enabling us to isolate single attosecond pulses. By using the appropriate optics this effect can be used to make a subperiod cut from the bulk pulse to obtain *isolated* subfemtosecond pulses.

It is crucial to operate in the λ^3 regime for the following reasons: (i) The driving beam should consist of well corrected and tightly focused fundamental frequency light, that allows one to limit wave front distortions and work with the *coherently* reflected radiation. (ii) Using only a few optical cycles makes possible a better discrimination between the initial collective action of electrons and their complex response to successive cycles. (iii) The narrow focus impresses a strong slope, increasing the angular separation of the reflected electromagnetic energy.

Two more effects should be mentioned. First, deformation of the plasma profile results in significant changes of the local incidence angle (defined to be the angle between the original wave front and the deformed reflecting surface). To enhance this effect the plasma density n_0 must be slightly overcritical, making the critical density surface more responsive to light pressure. Second, charge separation produces an electric field which is mostly normal to the plasma reflecting surface. Through these two effects we come to one more relativistic effect, which is the most important for us: along with the intense and coherent relativistic electron motion in the direction *perpendicular* to the wave vector of the reflected wave $\mathbf{k}_r$, which is responsible for the *magnitude* of the reflected wave, there must be also the coherent motion *parallel* to $\mathbf{k}_r$, which, according to the Doppler effect, should be responsible for dramatic *shortening or elongation* of the reflected pulse, depending on the sign of the parallel velocity.

Relativistic effects in supercritical plasmas have been discussed in their application to the generation of harmonics [11–13] and attosecond pulse trains [14] by weakly and tightly [13] focused long pulses. For the relativistic λ^3 regime discussed here, the Doppler phase compression becomes so significant that the reflected wave is disseminated in several pulses propagated in *different* directions, instead of being the quasiperiodic wave propagating in one direction.

To demonstrate this, we perform fully relativistic 2D PIC simulations, and study the highly nonlinear regime of the reflection. The PIC code integrates, self-consistently, Maxwell's equations and relativistic equations of motion for electrons and ions [15]. The computation box is $20\lambda \times 20\lambda$, with spatial resolution as high as 100 cells per λ. To resolve the density gradient we take 16 electrons and 16 ions per cell.

A linearly polarized laser pulse with its electric field along y direction has been initiated at the left boundary ($x = -14$) in vacuum and focused to a 1λ spot normal to the plasma layer. The laser pulse has a Gaussian profile and a duration equal to 5 fs ($\approx$2 cycles, full width at half maximum). The maximal intensity in the focus is $I = 2 \times 10^{19}$ W/cm^2. For $\lambda = 0.8$ μm this corresponds to the dimensionless amplitude $a_0 = 3$. The preionized plasma layer has a uniform profile, of thickness 2λ, and density $1.5n_{cr}$. The electron-ion collision frequency is negligible: $\nu_{ei} \approx 10^8$ s$^{-1} \ll \omega$. We choose $t = 0$ to be the instant when the peak of the pulse envelope reaches the plasma boundary at $x = 0$. Space coordinates are measured in laser wavelengths, and time in cycles.

In Fig. 1(a) the electromagnetic energy density is shown at $t = 11$ for $x < -1$. We see that the reflected radiation has been split into separate pulses, each moving in its own direction. The most intense pulse is located toward the upper left-hand corner of the box, the second most intense pulse is closer to the middle of the box, and the third and least intense pulse of the three is located toward the lower left-hand corner.

We plot the reflected radiation at the half-intensity level [Fig. 1(b)] and find that only a subperiod pulse has been reflected in the upward direction. We trace this pulse and find that it has a divergence of $\sim$20°. The maximum intensity values of this pulse follow a $\sim$40° direction with respect to normal incidence.

The evolution of the electron density [Fig. 1(c)] shows the motion of the reflecting surface driven by the laser pulse. Electron layers, pushed by the pulse, deflect each half-cycle into a new direction depending on the phase and amplitude of the particular half-cycle. In addition, the reflecting layer focuses these pulses in the backward direction with varying focal lengths. Thus, each cycle has its own divergence and its own virtual source point within the $\sim\lambda^3$ volume. Because of the very tight focus and short duration of the incident pulse this discrimination in the direction and curvature between separate cycles is possible. Figure 1(c) for $t = 1$ shows the surface, from which the pulse 1 has been reflected. The curvature, that reflects this pulse in the upward direction (pointed by an arrow), has the minimum focal length.

Our simulations show that the laser-plasma interaction is phase sensitive due to the short incident pulse duration.

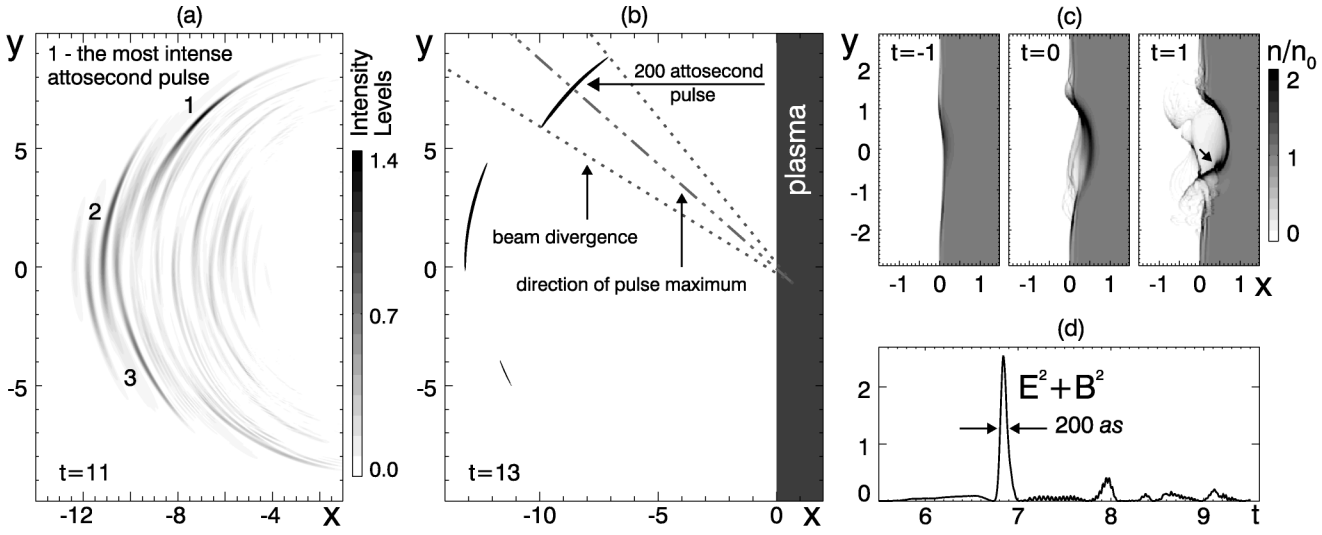

FIG. 1. Simulation parameters: $a = 3$, $\tau = 5$ fs, $n_0 = 1.5n_{cr}$. (a) The electromagnetic energy density of the reflected radiation ($E^2 + B^2$). Numbers 1, 2, 3 indicate the most intense pulses in the reflected radiation: 1 — with the highest intensity, 3 — with the lowest intensity of these three. (b) Half-intensity level of the reflected radiation. The horizontal arrow indicates a single attosecond pulse. The plasma layer is shown schematically. (c) Snapshots of the electron density. The arrow indicates the curvature from which the pulse 1 was reflected. (d) The time evolution of $E^2 + B^2$ at the point $x = -3.5$, $y = 3$. The arrows indicate the half-intensity level of an isolated pulse that contains 10% of the incident pulse energy.

Changing the phase of the pulse by π, we obtain a symmetrically mapped distribution for the reflected light, the most intense subperiod going to the lower left-hand corner.

We plot the time dependence of the electromagnetic energy density at the point $x = -3.5$, $y = 3$ in Fig. 1(d) (along the maximal intensity path of the pulse 1). We find that the duration of this pulse is only 200 attoseconds, yet it contains 10% of the incident pulse energy. The pulse has been compressed under the motion of the reflective layer of electrons in the direction parallel to $\mathbf{k}_r$.

The process of attosecond pulse formation also scales to higher energies. With an intensity increase of 2 orders of magnitude and plasma density increase of one order, substantially the same effect occurs and even shorter attosecond pulses are efficiently formed.

We performed 3D simulations in addition to 2D runs. The 3D results agreed with those in 2D geometry, with some natural differences due to the anisotropy caused by the polarization effects [16]. On the other hand, in 3D simulations it is presently hard to achieve higher spatial resolution, so the 2D result is more reliable.

An analytic model, presented for the sake of better clarity, involves only one nonlinear input to the component of the electron velocity, which is parallel to the plasma gradient, from the p-polarized electric field component of an incident plane wave. For short driving pulses the total electron displacement can be *negative*, from plasma towards the laser, resulting in an extremely sharp reflected pulse.

Let us consider the reflection of a short relativistically strong obliquely incident p-polarized plane electromagnetic pulse arriving at a foil. The angle of incidence, θ_0, is defined with respect to the x direction, the x axis being normal to the foil, the wave comes from the $x < 0$ half of space. The foil has thickness $l \ll \lambda$ and its density profile can be described by the Dirac delta function $n_e = N_0\delta(x)$. While calculating the charge motion we assume the fields created by the currents and charges in the foil to be small as compared to the fields in the incident wave. This is allowed by the following condition: $\epsilon_0 = 2\pi e^2 N_0/m_e\lambda \ll 1$ (see [12]). It is known that the problem for nonzero angle of incidence θ_0 can be reduced to the problem for $\theta_0 = 0$ [17] by using the reference frame K' which moves with the velocity as $V_y = c\sin\theta_0$, with respect to the original frame of reference K. In the K' frame the incident electric field has only one component E_y, the only component of the vector potential being A_y. Below our considerations are in the K' frame.

While in the original frame of reference K, the plasma was at rest in the absence of the incident wave, all the particles move with the velocity $-V_y$ in the K' frame. The Lorentz force which drives the electron in the x direction (normal to the foil), involves the term $-V_y B_z$, B_z being the wave magnetic field. The Lorentz force, and, consequently, the electron velocity, v_x, can be negative (directed outwards), so, the radiation field produced by the electron at that time has a shorter time scale due to the Doppler effect. In evaluating this effect, the conserved integrals of motion are $\kappa_y = p_y - eA_y/c = -m_e c\tan\theta_0$ and $\mathcal{E} = (m_e^2c^4 + p_x^2c^2 + p_y^2c^2)^{1/2} - p_x c = m_e c^2/\cos\theta_0$. These relations should be used while estimating the electron current $I_{y,e}$. The ion current in the frame of reference K' is $I_{y,i} = -eN_0V_y$.

In neglecting the radiation back reaction as well as the electron-ion interaction ($\epsilon_0 \ll 1$), the electron motion in the field of an arbitrary plane electromagnetic wave is given by well-known formulas, which describe this motion in a parametric form in terms of ξ, the parameter $2\pi\xi/\lambda$ being the phase of the wave (the incident wave in the present context) [18]:

$$x_e(\xi) = \int c p_x \mathcal{E}^{-1} d\xi, \qquad ct' = \xi + x_e(\xi), \tag{1}$$

$$p_x(\xi)/m_e c = \alpha(\alpha/2 - 1)\sin\theta_0\tan\theta_0, \tag{2}$$

$$v_x(\xi)/c = 1 - (1 + \alpha(\alpha/2 - 1)\sin^2\theta_0)^{-1}, \tag{3}$$

where $\alpha = a(\xi)/\tan\theta_0$, $a(\xi) = eA_y(\xi)/m_e c^2$. The longitudinal velocity v_x achieves the minimal value at $\alpha = 1$, if $a_0 = \max|a| > \tan\theta_0$.

We introduce here the time t' related to the electron motion to distinguish it from time t, which is used below to define the dimensional quantity associated with the phase of the reflected wave $\xi_r = ct + x$. The typical relation for the argument of the retarded potential is $ct + x = ct' + x_e(t')$, which allows us to relate the instant t, at which the retarded potential is determined at the point x [see below Eq. (4), note that $x < 0$ and that the reflected wave direction of propagation is opposite to the x-axis direction], to the instant t', when this reflected wave was actually emitted by the electron layer.

We find the vector potential in the reflected wave, by integrating the current:

$$\begin{aligned}\frac{A_r}{2\pi} &= \int_0^t d\tau \int_{-\infty}^{+\infty} d\eta [I_{y,e}\delta(\eta - x_e(\tau))\theta(\xi_r - c\tau - \eta) \\ &\qquad + I_{y,i}\delta(\eta)\theta(\xi_r - c\tau)] \\ &= \int_0^{t'} d\tau I_{y,e}(\tau) + I_{y,i}\xi_r,\end{aligned} \tag{4}$$

where $t'(\xi_r)$ is the solution of the equation as follows: $ct' = \xi_r - x_e(t')$, and $\theta(x)$ is the step function.

We use then, the relations: $\partial\xi/\partial t' = c - v_x(t')$, $\partial\xi_r/\partial t' = c + v_x(t')$, $\partial\xi_r/\partial\xi = 1 + 2cp_x\mathcal{E}^{-1}$, and finally find the electric field $E_{y,r}(\xi_r) = -\partial A_{y,r}/\partial\xi_r$ of the reflected wave in parametric form as follows (both $E_{y,r}$ and ξ_r are expressed in terms of ξ):

$$E_{y,r} = \frac{2\pi N_0 e(c\kappa_y + eA_y(\xi))\mathcal{E}}{m_e^2c^4 + (c\kappa_y + eA_y(\xi))^2} + \frac{2\pi N_0 e}{c}V_y, \tag{5}$$

$$\xi_r = \int [m_e^2c^4 + (c\kappa_y + eA_y(\xi))^2]\frac{d\xi}{\mathcal{E}^2}. \tag{6}$$

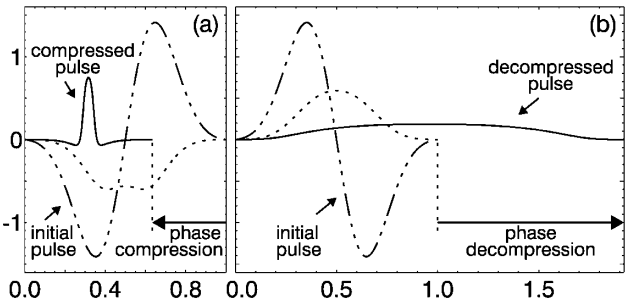

FIG. 2. The incident electric field $E(\xi)$ (dash-dotted line), electron velocity $v_x(\xi)$ (dotted line), and the reflected electric field $E_r(\xi_r)$ (solid line) for the parameters: $a_0 = 2.5$, $\theta_0 = \pi/3$, $\epsilon_0 = 0.5$ in the analytical model for the cases of pulse (a) compression and (b) decompression. The arrow shows the phase change for the reflected pulse: $-2\Delta x/\lambda$, where $\Delta x = x_e(\xi = 1)$.

The illustration of this analytical model for the initial pulse profile $E(\xi) = -a_0 \exp(-2(\xi/\lambda - 0.5)^2) \times \sin(2\pi\xi/\lambda)$, with parameters $a_0 = 2.5$, $\theta_0 = \pi/3$, and $\epsilon_0 = 0.5$ is shown in Fig. 2(a). We limit the incident electric field to one cycle, having in mind that the successive cycles create the reflection surfaces at different angles. Electron velocity v_x is negative, indicating that electrons move toward the pulse. Thus, the reflected pulse becomes much shorter due to the phase compression. On changing the sign of $E(\xi)$ in Fig. 2 the reflected pulse becomes longer due to the phase decompression.

Note that, just as in the numerical result, for short pulses, compression effects crucially depend on the relationship between the pulse phase and the incidence angle. On changing the sign of the electric field in the pulse at a fixed incidence angle, compression changes to decompression.

The suggested attosecond pulse generation scheme using supercritical plasma is several orders of magnitude more efficient than those involving recollisions in gas targets. This is because the ensemble effect of critical surface reflection, being coherent in nature, is near unity, while the cross section for recollision in gases is quite small.

With PIC simulation and analytical modeling we have shown that reflections in the relativistic λ^3 regime are accompanied by deflection and compression leading to the generation of isolated attosecond pulses with $\sim 10\%$ efficiency. This technique can be scaled from the millijoule to the joule level.

We are thankful to S.V. Bulanov for useful discussions. The work was supported by the NSF Grant No. 0114336.

*Also at General Physics Institute RAS, Vavilov Str. 38, Moscow 119991, Russia.
†Electronic address: mourou@eecs.umich.edu

[1] P. B. Corkum, Phys. Rev. Lett. **71**, 1994 (1993).
[2] M. Hentschel, R. Kienberger, Ch. Spielmann, G. A. Reider, N. Milosevic, T. Brabec, P. Corkum, U. Heinzmann, M. Drescher, and F. Krausz, Nature (London) **414**, 509 (2001); R. Kienberger, M. Hentschel, M. Ulberacker, Ch. Spielmann, M. Kitzler, A. Scrinzi, M. Wieland, Th. Westerwatbesloh, U. Kleineberg, U. Heinzmann, M. Drescher, and F. Krausz, Science **297**, 1144 (2002).
[3] A. Paul, R. A. Bartels, R. Tobey, H. Green, S. Weiman, I. P. Christov, M. M. Murnane, H. C. Kapteyn, and S. Backus, Nature (London) **421**, 51 (2003).
[4] D.-F. Liu, J. Nees, H.-W. Wang, G. Mourou, Z. Chang, and O. Albert, in *Conference on Lasers and Electro-Optics (CLEO)*, Postconference Digest, OSA Trends in Optics and Photonics Vol. 39 (Optical Society of America, Washington, DC, 2000), p. 662.
[5] O. Albert, H. Wang, D. Liu, Z. Chang, and G. Mourou, Opt. Lett. **25**, 1125 (2000).
[6] A. G. Litvak, Zh. Eksp. Teor. Fiz. **57**, 629 (1969); Sov. Phys. JETP **30**, 344 (1969).
[7] C. Max, J. Arons, and A. B. Langdon, Phys. Rev. Lett. **33**, 209 (1974).
[8] A. B. Borisov, A.V. Borovskiy, O. B. Shiryaev, V.V. Korobkin, A. M. Prokhorov, J. C. Solem, T. S. Luk, K. Boyer, and C. K. Rhodes, Phys. Rev. A **45**, 5830 (1992).
[9] P. Monot, T. Auguste, P. Gibbon, F. Jakober, and G. Mainfray, Phys. Rev. Lett. **74**, 2953 (1995).
[10] G. Mourou, Z. Chang, A. Maksimchuk, J. Nees, S.V. Bulanov, V.Yu. Bychenkov, T. Zh. Esirkepov, N. M. Naumova, F. Pegoraro, and H. Ruhl, Plasma Phys. Rep. **28**, 12 (2002).
[11] S.V. Bulanov, N. M. Naumova, and F. Pegoraro, Phys. Plasmas **1**, 745 (1994); R. Lichters, J. Meyer-ter-Vehn, and A. M. Pukhov, Phys. Plasmas **3**, 3425 (1996).
[12] V. A. Vshivkov, N. M. Naumova, F. Pegoraro, and S.V. Bulanov, Phys. Plasmas **5**, 2727 (1998).
[13] S.V. Bulanov, T. Zh. Esirkepov, N. M. Naumova, and I.V. Sokolov, Phys. Rev. E **67**, 016405 (2003).
[14] L. Roso, L. Plaja, K. Rzazewski, and D. von der Linde, Laser Part. Beams **18**, 467 (2000).
[15] C. K. Birdsall and A. B. Langdon, *Plasma Physics via Computer Simulation* (McGraw-Hill, New York, 1985).
[16] N. M. Naumova, S.V. Bulanov, K. Nishihara, T. Zh. Esirkepov, and F. Pegoraro, Phys. Rev. E **65**, 045402 (2002).
[17] A. Bourdier, Phys. Fluids **26**, 1804 (1983).
[18] L. D. Landau and E. M. Lifshits, *The Classical Theory of Fields* (Pergamon, Oxford, 1983).